Supplementary information

Quantitative measurement of macromolecular tissue properties in white and gray matter in healthy aging and amnestic MCI

Elveda Gozdas[1], Hannah Fingerhut[1], Hua Wu[2], Jennifer L. Bruno[1], Lauren Dacorro[1], Booil Jo[1], Ruth O'Hara[1], Allan L. Reiss[1], S.M. Hadi Hosseini[1]

[1] Department of Psychiatry and Behavioral Sciences, Stanford University School of Medicine, Stanford, CA

[2]Center for Cognitive and Neurobiological Imaging, Stanford University, Stanford, CA

Supplemental Data

Table S1. Demographic, clinical and neuropsychological characteristics of the sample

	HC N=45	**aMCI N=19**	**Statistics***
Age, years (SD)	73.5(5.9)	73.6(5.5)	*p*=0.97
Gender (F/M)	32/13	8/11	*p=0.047*
Years of Education (SD)	17.88(3.5)	18.55(3)	*p*=0.44
MMSE (SD)	28.97(1.05)	27.26(1.7)	*p=0.0005*
ICV (SD)	1396.8(120.1)	1462.2(136.8)	*p=0.34*
SDMT (SD)	71.66(16.8)	58.7(9.8)	*p=0.001*
PSMT (SD)	9.66(5.7)	5.5(4.3)	*p=0.017*
Rey (SD)	22.02(5)	17.9(5.5)	*p=0.008*

* p values derived from two-sample t-test, Chi-square test or ANOVA with age, gender, education and intracranial volume as covariates.

HC: Healthy Control; aMCI: amnestic Mild Cognitive Impairment; MMSE: Mini-Mental State Examination; ICV: intracranial volume (cm^3); SDMT: Symbol Digit Modalities Test; PSMT: Picture Sequence Memory Test; Rey: Auditory Verbal Learning Test

Table S2. Statistics for age association for each three white matter measures

WM Microstructure	Tract	Mean (SD)	β	p (FDR corrected)
MTV				
	Left Thalamic Radiation	0.274(0.009)	-0.2569	0.16285714
	Right Thalamic Radiation	0.2737(0.01)	-0.14	0.01827931
	Left Corticospinal	0.275(0.007)	-0.37416574	0.095
	Right Corticospinal	0.275(0.008)	-0.37682887	0.04238462
	Left Cingulum Cingulate	0.271(0.011)	-0.4494441	0.03081081
	Right Cingulum Cingulate	0.273(0.01)	-0.40249224	0.03081081
	Left Cingulum Hippocampus	0.246(0.014)	-0.36742346	0.03081081
	Right Cingulum Hippocampus	0.249(0.017)	-0.24899799	0.16285714
	Callosum Forceps Minor	0.256(0.04)	-0.54221767	0.05004878
	Left IFOF	0.267(0.01)	-0.6	0.00095
	Right IFOF	0.266(0.01)	-0.59160798	0.00095
	Left ILF	0.271(0.009)	-0.4472136	0.036
	Right ILF	0.271(0.01)	-0.50990195	0.0285
	Left SLF	0.281(0.009)	-0.46904158	0.0095
	Right SLF	0.282(0.009)	-0.41231056	0.0285
	Left Uncinate	0.240(0.013)	-0.5	0.67363636
	Right Uncinate	0.238(0.01)	-0.54772256	0.03081081
	Left Arcuate	0.289(0.009)	-0.51961524	0.0095
	Right Arcuate	0.286(0.012)	-0.4	0.00316667
MD				
	Left Thalamic Radiation	0.918(0.08)	0.5	0.0019
	Right Thalamic Radiation	0.913(0.08)	0.54772256	0.0007125
	Left Corticospinal	0.915(0.05)	0.4472136	0.00673636
	Right Corticospinal	0.928(0.05)	0.47958315	0.00488571
	Left Cingulum Cingulate	0.869(0.03)	0.54772256	0.00095
	Right Cingulum Cingulate	0.869(0.04)	0.56568542	0.000627
	Left Cingulum Hippocampus	0.935(0.05)	0.46904158	0.004275
	Right Cingulum Hippocampus	0.964(0.06)	0.51961524	0.00204529
	Callosum Forceps Minor	1.012(0.07)	0.45825757	0.01604444
	Left IFOF	0.984(0.08)	0.64031242	0.00008835
	Right IFOF	1.004(0.09)	0.70569115	0.00001539
	Left ILF	0.979(0.06)	0.6164414	0.0001425
	Right ILF	0.997(0.06)	0.70710678	0.0000456
	Left SLF	0.872(0.05)	0.54772256	0.00095
	Right SLF	0.881(0.05)	0.51961524	0.0019

	Left Uncinate	0.934(0.06)	0.42426407	0.01512692
	Right Uncinate	0.936(0.05)	0.65574385	0.0000456
	Left Arcuate	0.891(0.05)	0.54772256	0.00100846
	Right Arcuate	0.905(0.05)	0.4	0.01771071
FA				
	Left Thalamic Radiation	0.325(0.027)	-0.29495762	0.25811321
	Right Thalamic Radiation	0.329(0.028)	-0.39496835	0.12286667
	Left Corticospinal	0.425(0.018)	-0.26832816	0.69214286
	Right Corticospinal	0.411(0.018)	-0.17888544	0.97
	Left Cingulum Cingulate	0.300(0.027)	-0.232379	0.171
	Right Cingulum Cingulate	0.287(0.027)	-0.22135944	0.39055556
	Left Cingulum Hippocampus	0.257(0.027)	-0.36055513	0.03081081
	Right Cingulum Hippocampus	0.270(0.031)	-0.25099801	0.14553192
	Callosum Forceps Minor	0.341(0.046)	-0.42426407	0.10604651
	Left IFOF	0.298(0.026)	-0.42661458	0.01368
	Right IFOF	0.290(0.022)	-0.62289646	0.0001425
	Left ILF	0.247(0.017)	-0.41231056	0.0285
	Right ILF	0.239(0.017)	-0.50990195	0.001995
	Left SLF	0.223(0.016)	-0.26457513	0.11011364
	Right SLF	0.234(0.018)	-0.31622777	0.049875
	Left Uncinate	0.246(0.025)	-0.41231056	0.12391304
	Right Uncinate	0.261(0.030)	-0.53851648	0.0033
	Left Arcuate	0.234(0.018)	-0.29154759	0.17538462
	Right Arcuate	0.221(0.020)	-0.2258318	0.17538462

Figure S1. Heatmap of inter- and intra-hemispheric association (Pearson's r) among MTV, FA, MD, RD and AD

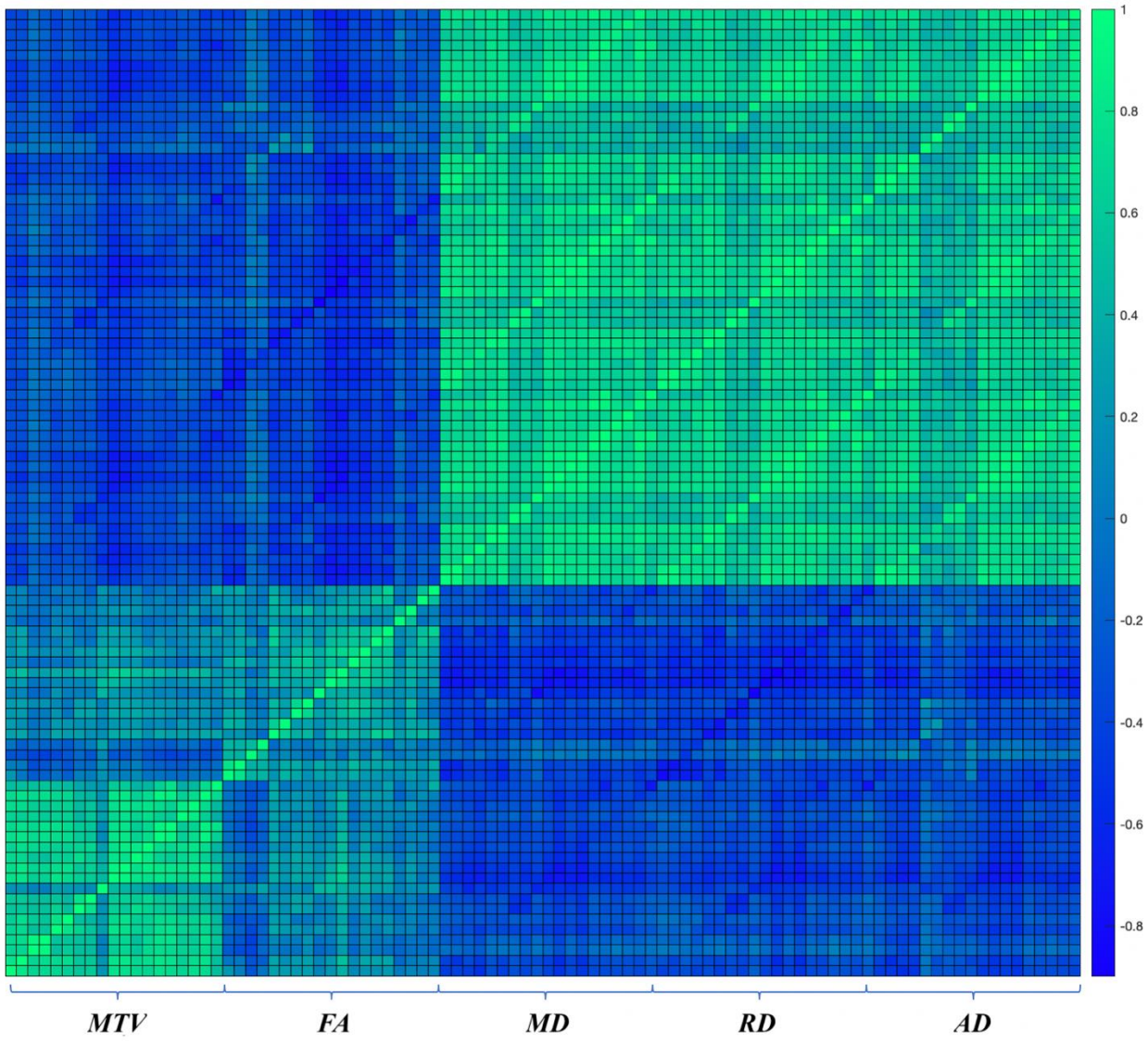

Figure S2. Association between volumetric brain MRI measures and age.

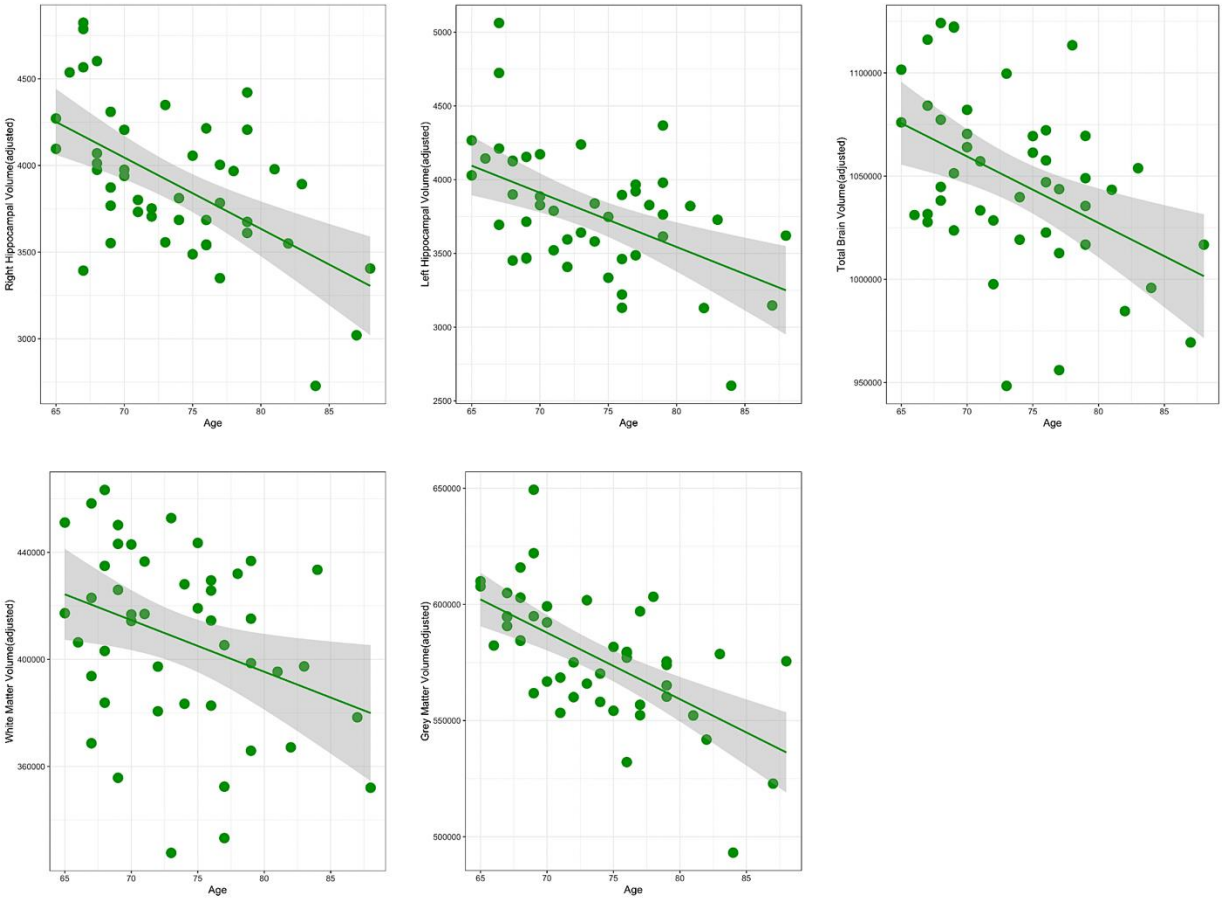

Supplemental Methods

Participants

Exclusion criteria for all participants included left-handedness, presence of suicidality, formal diagnosis of a significant psychiatric disease, current regular use of psychotropic medications, opiates, or thyroid medications (except for permitted medications including cholinesterase inhibitors and hypertension medications if stable for at least two months), claustrophobia, non-MRI-compatible materials, post-traumatic or psychotic disorders, bipolar disorder; any

significant neurologic disease including possible and probable dementia, multi-infarct dementia, Parkinson's or Huntington's disease, brain tumor, progressive supranuclear palsy, seizure disorder, subdural hematoma, multiple sclerosis, "uncontrolled" hypertension, history of significant head trauma, current or history of alcohol or substance abuse or dependence within the past 2 years; any significant systemic or unstable medical condition.

Eligible participants underwent a battery of neuropsychological assessments to be included in the study.

Cognitive Measures

The NIH Toolbox Cognition Battery was administered using an iPad (www.nihtoolbox.org). The battery comprised of several tests including the Picture Sequence Memory Test (PSMT) (Boake, 2000) for assessing episodic memory, Auditory Verbal Learning Test (Rey) (Dikmen, 2014) for testing memory recall and Symbol Digit Modalities Test (SDMT) (Weintraub et al., 2013) for assessing processing speed. The PSMT involved presentation of sequences of pictured objects and activities in a fixed order on the iPad screen and simultaneously verbally described. The participant must remember and then reproduce the sequences over three trials. Scores on these measures are strongly correlated to scores from well-established "gold standard" measures of episodic memory. The Rey test involves auditory presentation of a list of unrelated words and asking participants to immediately recall as many words as possible following the presentation of the words. The SDMT consists of a series of nine symbols presented at the top of a standard sheet of paper, each paired with a single digit. The rest of the sheet contains symbols not matched to a digit, and participants were asked to say the digit corresponding with each symbol as quickly as possible and without making mistakes. The resulting score is equal to the number of correct matches over a period of 120 seconds.

dMRI acquisition and processing

Multi-shell dMRI were acquired for all participants, with isotropic 2 mm^3 spatial resolution. The pulse sequence included 119 total directions comprising 80 diffusion gradient directions with b=2855 s/mm^2, 30 diffusion gradient directions with b=710 s/mm^2 and nine images without diffusion weighting (b=0 s/mm^2). To facilitate EPI distortion correction an additional scan was acquired in the opposite phase encoding direction and included 6 diffusion gradient directions (b=2855 s/mm^2) and two non-diffusion-weighted images. Other dMRI parameters are as follows: TR/TE=2800/78ms, FOV=22.4cm, matrix size=112x112, and 63 axial slices with simultaneous multi-slice acceleration factor of 3. T1-weighted images were acquired in the sagittal plane using a three-dimensional GE BRAVO sequence at a resolution of 1x1x1 mm, with 256x256 field of view. Intracranial brain volume for all participants was calculated on T1-weighted images using the FreeSurfer Software Suite, version 6.0 (http://surfer.nmr.mgh.harvard.edu/). dMRI data preprocessing was implemented in FSL (fsl.fmrib.ox.ac.uk/fsl/fslwiki/) and MRTrix3(mrtrix.org) and included denoising, geometric EPI distortion, eddy current distortion, slice-by-slice motion correction, outlier detection and bias field correction (ANTs N4BiasField Correction). Diffusion gradients were then adjusted to account for the rotation applied to the measurements during motion correction and a tensor model was fit for each voxel's data using the diffusion kurtosis (DK) model. DK is an extension of the diffusion tensor model that accounts for the non-Gaussian behavior of water in heterogeneous tissue containing multiple barriers to diffusion and it may be useful for investigating neurodegenerative diseases (Jensen and Helpern, 2010). To quantify the potential effects of motion, the participants with mean slice-by-slice root mean square displacement >1.5mm were excluded from the analysis. We also tested for differences in motion across groups

and observed no group differences between aMCI and control groups. Multi-tissue constrain spherical deconvolution was used to estimate the fiber orientation distributions (FODs) on aligned and distortion corrected dMRI data using average tissue response function. Probabilistic tractography was performed in MRtrix (3.0) using white matter FOD images to generate a whole-brain connectome for each subject.

White matter tract identification

The Automated Fiber Quantification (AFQ, v1.1, github.com/yeatmanlab/AFQ/wiki) (Yeatman et al., 2012; Huber et al., 2018) software package was used to segment the whole brain connectome of fiber tracts and quantify tissue properties along each tract. AFQ uses a two way-point ROI procedure to define 19 white matter tracts in which each fiber from the whole-brain connectome becomes a candidate for a specific fiber group if it passes through two ROIs that define the trajectory of the fiber group (Wakana et al., 2004). Next, each candidate fiber that passes through regions of the white matter that are unlikely to be part of the tract was removed to define only the tract fibers at the central position and fibers with length greater than three standard deviations from the mean fiber length were removed. The diffusion metrics (FA, MD, AD and RD) were then projected onto the segmented white matter fibers generated by AFQ. The FA and MD metrics describe the directional coherence and magnitude of water diffusion, respectively. FA (dimensionless index) is increased when water molecules tend to diffuse with greater directional coherence in the presence of well-myelinated axons. Tissue loss lowers the local barriers to the movement of water molecules that causes an increase in the magnitude of diffusion, and MD ($\mu m^2/s$) is increased. AD ($\mu m^2/s$) and RD ($\mu m^2/s$) refer to the magnitude of water diffusion parallel and perpendicular to fiber tracts, respectively.

Validation of the qT1 Sequence

The qT1 measurements have been previously validated against the standard IR spin-echo EPI sequence (Mezer at al., 2013). The figures below show a comparison of the whole brain qT1 measurements between the two methods. We see a good correspondence of the T1 values, particularly in the gray matter and white matter. The mean T1 is 1392.9 (117.2) ms and 980.4 (99.0) ms with the qT1 sequence, versus 1387.6 (153.6) ms and 974 (101.4) ms with the IR EPI sequence. The overall Pearson's correlation coefficient between the two datasets is 0.82, with an RMSE of 216 ms.

Figure S3. T1 map of a single subject using the qT1 sequence (top row) and the standard IR spin-echo EPI sequence (bottom row).

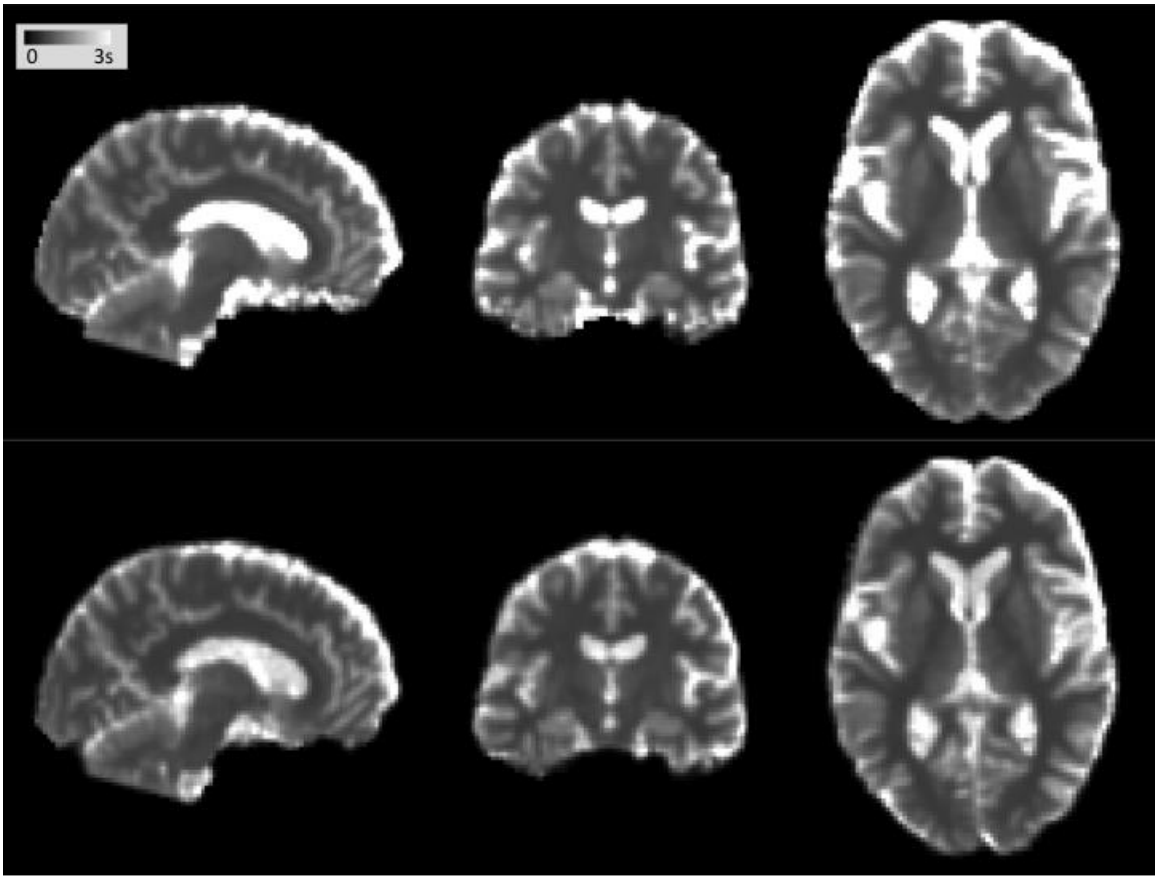

Figure S4. Correlation between the measured T1 values using the qT1 sequence and the standard IR spin echo EPI sequence.

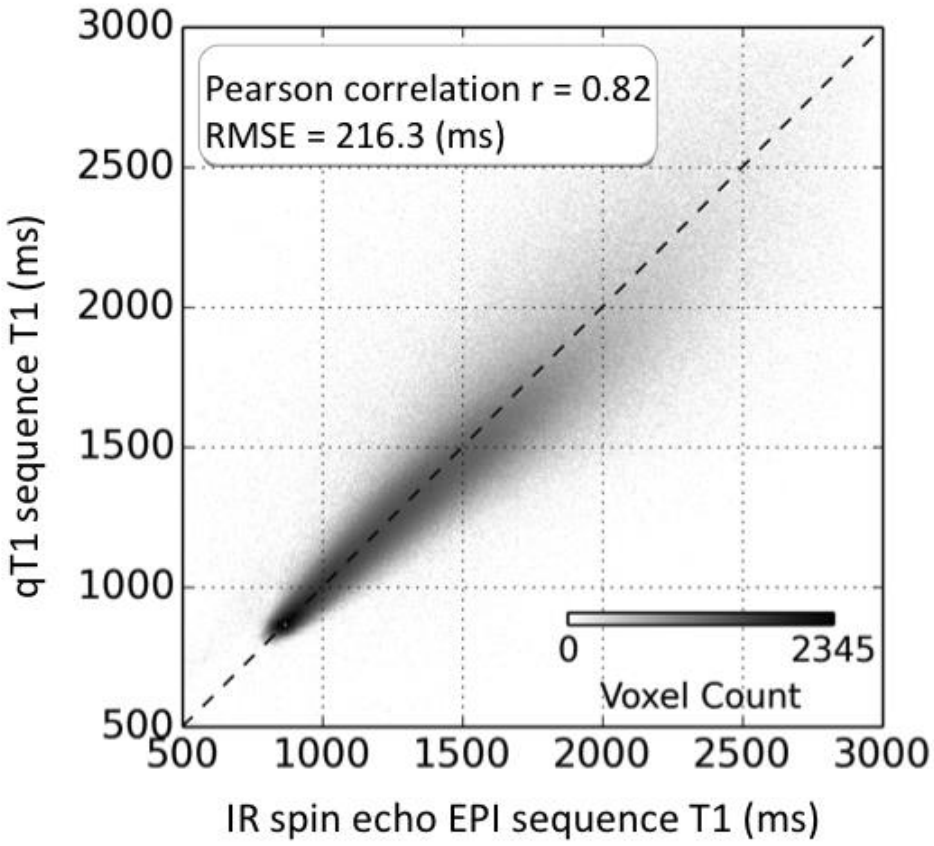

Supplemental References

Boake, C., 2000. Edouard Claparede and the auditory verbal learning test. Journal of Clinical and Experimental Neuropsychology 22, 286-292.

Dikmen, S.S., Bauer, P.J., Weintraub, S., Mungas, D., Slotkin, J., Beaumont, J.L., Gershon, R., Temkin, N.R., Heaton, R.K., 2014. Measuring episodic memory across the lifespan: NIH toolbox picture sequence memory test. Journal of the International Neuropsychological Society: JINS 20, 611.

Huber, E., Donnelly, P.M., Rokem, A., Yeatman, J.D., 2018. Rapid and widespread white matter plasticity during an intensive reading intervention. Nature communications 9, 1-13.

Jensen, J.H., Helpern, J.A., 2010. MRI quantification of non- Gaussian water diffusion by kurtosis analysis. NMR in Biomedicine 23, 698-710.

Mezer, A., Yeatman, J.D., Stikov, N., Kay, K.N., Cho, N.-J., Dougherty, R.F., Perry, M.L., Parvizi, J., Hua, L.H., Butts-Pauly, K., 2013. Quantifying the local tissue volume and composition in individual brains with magnetic resonance imaging. Nature medicine 19, 1667-1672.

Wakana, S., Jiang, H., Nagae-Poetscher, L.M., Van Zijl, P.C., Mori, S., 2004. Fiber tract–based atlas of human white matter anatomy. Radiology 230, 77-87.

Weintraub, S., Dikmen, S.S., Heaton, R.K., Tulsky, D.S., Zelazo, P.D., Bauer, P.J., Carlozzi, N.E., Slotkin, J., Blitz, D., Wallner-Allen, K., 2013. Cognition assessment using the NIH Toolbox. Neurology 80, S54-S64.

Yeatman, J.D., Dougherty, R.F., Myall, N.J., Wandell, B.A., Feldman, H.M., 2012. Tract profiles of white matter properties: automating fiber-tract quantification. PloS one 7, e49790.